J Mater Sci: Mater Med (2010) 21:635–646
DOI 10.1007/s10856-009-3886-y

The biocompatibility of sulfobetaine engineered polymethylmethacrylate by surface entrapment technique

Anand P. Khandwekar · Deepak P. Patil · Yogesh S. Shouche · Mukesh Doble

Received: 11 June 2009 / Accepted: 30 September 2009 / Published online: 11 October 2009

Abstract Sulfobetaine-modified polymethylmethacrylate (PMMA) systems were created by physically entrapping the zwitterionic species on the PMMA surface. The presence of the sulfobetaine molecules on these surfaces were verified by ATR–FTIR and SEM–EDAX analysis, while wettability of the films was investigated by dynamic contact angle measurements. The short-term (4 h) adhesion of two bacterial species (gram-positive *Staphylococcus aureus* and gram-negative *Pseudomonas aeruginosa*) on these surfaces were studied. Mouse RAW 264.7 macrophage cells were used to assess the cell adhesion and inflammatory response by quantifying the expression levels of pro-inflammatory cytokines namely TNFα and IL1β by measuring their mRNA profiles in the cells using real-time polymerase chain reaction (RT-PCR) normalized to the house keeping gene GAPDH. Whilst mouse L-929 fibroblast cells were used to assess the propensity for the materials to support fibroblast cell adhesion. A decrease in the adhesion of *S. aureus* by 63% and *P. aeruginosa* by 49% was observed on sulfobetaine modified PMMA films after 4 h. In all the cases, sulfobetaine modified PMMA films reduced cellular adhesion events ($^{*}P < 0.05$) with respect to the base materials, which could be linked to the reduced protein adsorption observed on these surfaces. The cellular inflammatory response was suppressed on sulfobetaine modified substrates as expression levels of pro-inflammatory cytokines (TNFα and IL1β) was found to be up regulated on bare PMMA, while it was significantly lower on sulfobetaine modified PMMA ($^{**}P < 0.001$). Thus the sulfobetaine entrapment process can be applied on polymethylmethacrylate in order to achieve low biointeractions and reduced inflammatory host responses for various biomedical and biotechnological applications.

Electronic supplementary material The online version of this article (doi:10.1007/s10856-009-3886-y) contains supplementary material, which is available to authorized users.

A. P. Khandwekar · M. Doble (✉)
Department of Biotechnology, Indian Institute of Technology Madras, Chennai 600036, India
e-mail: mukeshd@iitm.ac.in

A. P. Khandwekar
e-mail: anandkhandwekar@gmail.com

D. P. Patil · Y. S. Shouche
National Center for Cell Science, Ganeshkhind, Pune 411007, India

1 Introduction

Polymers are widely used in the biomedical field for the fabrication of medical implants and devices, including vascular, orthopedic and ophthalmologic implants [1]. Historically, materials have been selected on the basis of their mechanical and physical properties rather than their biological performance. For example, medical device associated infections have become a growing problem with the increased utilization of these devices [2]. In many biomedical applications the adhesion of proteins, cells and bacteria to biomaterials causes undesirable inflammation or infection. Also, the inflammatory host responses to implanted biomaterials limit device integration and biological performance for most classes of medical devices [3]. These inflammatory responses to synthetic materials involve dynamic, multi-component and interdependent reactions comprising biomolecule (e.g., protein) adsorption, leukocyte recruitment, adhesion and activation, cytokine expression/release, macrophage fusion into multinucleated foreign body giant cells, tissue remodeling and fibrous encapsulation [4, 5]. The duration and intensity

of these stages are dependent upon the extent of injury created at the implantation site and the biomaterial physicochemical properties [4].

In recent years various research groups have therefore focused on the development of bioinert, biocompatible coatings which can be used to minimize protein adsorption and cellular adhesion whilst maintaining the mechanical and physical properties of the underlying substrate [6]. The attachment of bacteria to materials is biologically significant as it can cause postoperative infection of medical implants, and subsequent implant failure. *Staphylococcus aureus* and *Pseudomonas aeruginosa* are two key organisms associated with implant infections [1, 7]. In vivo bacterial adhesion to materials follows initial conditioning of the material with proteins found in bodily fluids [8]. Bacteria adhere to these bound proteins and create microcolonies which ultimately fuse to form biofilms [9] Studies of polymeric materials have shown that 81% of infections are caused by *Staphylococcus* [10]. Most of the *Staphylococcus* sp. are also known to increase the adherence of the opportunistic bacteria *P. aeruginosa* and *Proteus mirabilis* [7, 11, 12].

PMMA has been selected as a model substrate because of its recurrent use in clinical applications. PMMA finds large use in many applications particularly in the orthopedic field as bone cement and in ophthalmology as artificial intraocular lenses (IOLs). As a well known fact biomedical devices manufactured from PMMA are prone to non specific bacterial/cellular adhesion events [13]. Postoperative endophthalmitis after intraocular lens (IOL) implantation is still one of the most fearsome complications of cataract surgery. Bacterial/cellular adhesion and activation to IOLs during insertion is believed to represent a prominent etiological factor in postoperative endophthalmitis and in pseudophakic chronic intraocular inflammation [14, 15]. Thus, reducing these nonspecific adhesion events to PMMA would possibly decrease the incidence of these diseases.

The lipid components that constitute the cytoplasm membrane are mainly zwitterionic phospholipids and are biocompatible in nature [16, 17]. Previously, polymers with phospholipid headgroups have been shown to have excellent biocompatible properties since the phosphorylcholine (PC) group mimics the outer cell membrane [18–21]. Polymers with phospholipid groups have no effect on epithelial cell migration, and show low cell adhesion [22]. Recently, sulfobetaine structures have received increased attention to become one of the most representative structures in the well-identified class of polymeric zwitterionic materials [23–26].

However, there are very few reports available in the literature regarding surface modification of polymethylmethacrylate (PMMA) with zwitterionic species and the effect of these zwitterionic coatings in the context of their antibioadherence capacity. Previously, we reported a surface entrapment technique as an effective strategy for surface modification of biomedical polymers like polyurethane and poly (ethylene terephthalate) [27–29]. In present study, polymethylmethacrylate surfaces were engineered by surface entrapment of the sulfobetaine species during the reversible swelling of the polymer surface region. The entrapment technique followed in the present work does not involve any toxic reagents but uses only aqueous solutions and also follows mild reaction conditions. Surface changes after the modification process were extensively probed with several spectroscopic and microscopic analytical techniques. The biocompatibility of sulfobetaine engineered PMMA was evaluated by their relative resistance to protein adsorption, bacterial and cellular adhesion events. The pro-inflammatory cytokines tumor necrosis factor (TNF-α) and interleukin (IL1-β) are known to be two of the most important signaling molecules involved in conducting the response to foreign materials, and their upregulation is considered to be an accurate measure of inflammation [30]. Genetic regulation precedes protein production, and in the current studies the changes in TNF-α and IL1β transcript levels were quantified using real-time reverse transcription polymerase chain reaction (RT-PCR). Real-time polymerase chain reaction is an in vitro method for enzymatically amplifying defined sequences of RNA [31]. Furthermore, it is the most sensitive, accurate, and adaptable of mRNA quantitative techniques. Thus, in this study by using sulfobetaine as a surface modifier the potential of sulfobetaine modified PMMA was evaluated in creating a biocompatible/cell-non-adhesive surface capable of reducing bacterial, cellular adhesion and inflammatory responses for future tissue contacting applications of PMMA such as that for Intraocular lenses (IOLs) and other biomedical applications were non specific adhesion events are not desired.

2 Materials and methods

2.1 Surface entrapment process

PMMA (medium mol wt., Alfa Aesar Co.) was obtained in the form of powder. A solution of PMMA in Acetone (Merck) at 50 mg/ml was used to cast films of 1.5 mm wet thickness using a casting knife. These casted films were cured for 6 h in an oven at 60°C to evaporate the solvent. Acetone was used as a modification solvent for PMMA and it was found that a dilution of acetone to 65% with deionized filtered water (DIFW) was suitable for the entrapment procedure. The surface modifying solution was

then prepared by first dissolving stearyl sulfobetaine (Sigma) in DIFW, and then adding acetone to it. The resultant mixture consisted of 10% (w/v) stearyl sulfobetaine, 65% (v/v) acetone and 25% (v/v) deionized filtered water (DIFW). PMMA films were immersed in 10 ml of this solvent/nonsolvent mixture for 1 h, with periodic swirling, finally the solution was quenched with an excess of nonsolvent (~20 ml DIFW) and the treated films transferred to water for storage. A solvent control was also run with same acetone dilution (65% acetone but without stearyl sulfobetaine) that creates the same degree of surface swelling, to account for possible residual solvent effects on various biological interactions.

2.2 Physical adsorption

The PMMA films were incubated with 10% (w/v) of stearyl sulfobetaine in PBS pH 7.4 at 37°C for 1 h. Following the treatment, samples were gently washed once in PBS.

2.3 Surface characterization

Surface analysis was performed with various spectroscopic and microscopic analytical techniques mentioned below. Hereby, for convenience polymethylmethacrylate, solvent treated polymethylmethacrylate and sulfobetaine modified polymethylmethacrylate will be abbreviated as PMMA, PMM-AC and PMMA-SB respectively.

2.3.1 Attenuated total reflection-Fourier transform infrared spectroscopy (ATR)–FTIR

ATR–FTIR spectra of the base and modified PMMA samples were obtained using FT/IR-4200 (Jasco, Netherlands) spectrometer having a baseline horizontal ATR accessory. Films were pressed against Zn-Se crystal and the spectra were collected at a resolution of 4 cm^{-1}.

2.3.2 Dynamic contact-angle and surface free energy measurements

The hydrophobicity and heterogeneity of the polymer surfaces were determined by advancing and receding contact angle measurements using a Kruss Easy drop goniometer (KRUSS, DSA II GmbH, Germany). Ultrapure water was used as the contact angle liquid, and the measurements were carried out on at least five independent specimens.

The surface free energy of the samples were calculated using Fowkes's method [32], based on measurements using three probe liquids, namely Diiodomethane (Sigma), Formamide (Sigma) and Water (Ultrapure).

2.3.3 Scanning electron microscopy and energy dispersive X-ray analysis (SEM–EDAX)

Energy dispersive X-ray analysis was performed to identify and quantify the elemental composition on the surfaces with the help of a FEI scanning electron microscope (Model Quanta 200, USA). The analysis was performed at 20 keV beam acceleration voltages with analysis time of 100 s. The ZAF program, which does not require the presence of any internal standard, was used to calculate the elemental composition of the surface [33, 34].

2.3.4 Scanning electron microscopy investigation of the entrapment structure

To characterize the surface structure of entrapped sulfobetaine molecules on surface of PMMA films, the specimen was investigated using a scanning electron microscopy (JEOL JSM 6380, Japan). Images were collected as a stack of 2-dimensional optical sections by digitizing sequential series of images while focusing down through the specimen.

2.3.5 Stability of surface films

The stability of the sulfobetaine entrapped PMMA films were investigated and was compared with that of physically adsorbed PMMA. The PMMA substrates (Physically adsorbed and surface entrapped sulfobetaine species) were subjected to stability analysis along with the control PMMA by ultra sound treatment [35]. Briefly, polymer films were dried and subsequently their static contact angles were noted. The films were then sonicated for 3 min followed by contact angle measurements. This cycle was repeated after gaps of 1 h each during which period the films were equilibrated with water at 37°C. The variation of water contact angle with the number of cycles was monitored, which was taken as a measure of stability of the modified films.

2.4 Protein adsorption

Bovine fibrinogen (Himedia, India) was obtained as lyophilized powder. The buffer solution used in the protein adsorption experiments was phosphate buffered saline (PBS, pH 7.4). Quantification of adsorbed protein on the polymer surfaces was performed using ^{125}I-labelled protein. ^{125}I-labelled protein was added to unlabelled protein solution in order to obtain a final activity of approximately 10^7 cpm/mg. The samples were immersed into 1 ml buffer solution at 37°C, and then 1 ml fibrinogen solution (0.2 mg/ml) was added and mixed. Adsorption tests were carried out at 37°C during 1 h. After protein adsorption, samples

were rinsed three times with 2 ml of buffer solution. The gamma activities were counted with the samples placed in radio-immunoassay tubes by a Gamma Counter. The counts from each sample were averaged and the surface concentration was calculated from the following equation:

$$\text{BFG}\left(\mu g/cm^2\right) = \text{Counts (cpm)}\ C_{\text{solution}}\ (\mu g/ml)/ [A_{\text{solution}}\ (\text{cpm/ml}) \times S_{\text{sample}}\ (cm^2)]$$

where the Count measures the radioactivity of the samples, the S_{sample} measure the surface area of the samples, C_{solution} and A_{solution} are the concentration and the specific activity of the protein solution, respectively. Statistical significance was ascertained by Student's t test and the data was expressed as means and SD from a single experiment performed in triplicates, which was representative of three independent experiments ($n = 3$ in each group).

2.5 Short-term bacterial adhesion assays

The initial short-term (4 h) adhesion of two bacterial species involving both gram-positive *S. aureus* (NCIM 5021) and gram-negative *P. aeruginosa* (NCIM 5029) were studied to understand the potential of these materials to resist/inhibit bacterial adhesion/biofilm formation. Hundred millilitres of nutrient broth (Himedia, India) was inoculated with a single colony of bacteria from a tryptone soya agar (Himedia, India) stock plate. The broth was incubated at 37°C overnight in a shaking incubator. The broth was split between 2 falcon tubes and centrifuged at 3500 rpm for 20 min. Cells were resuspended in phosphate buffered saline (PBS, pH 7.4). This was repeated twice more and cells were finally resuspended at a concentration of 1×10^8 cells/ml. Polymer discs were placed in a 24 well plate. Discs were incubated in 1 ml of the 1×10^8 cells/ml for 4 h at 37°C in a shaking incubator, rinsed in twice with PBS, then the bacteria were eluted from the surfaces into 2 ml sterile PBS using an ultrasonic cleaner (Perkin Elmer, USA) which involves 4 min sonication followed by 1 min mild vortexing (three times). A known volume of the sample was inoculated onto tryptone soya agar and incubated at 37°C for 24 h. The colony forming units were counted and the total number of bacteria retained calculated. Statistical significance was ascertained by Student's t test and the data was expressed as means and SD from a single experiment performed in triplicates, which was representative of three independent experiments ($n = 3$ in each group).

2.6 Cell culture studies

Mouse L-929 fibroblasts and RAW 264.7 macrophage cell lines were obtained from NCCS, Pune (India) and maintained in Dulbecco's modified Eagle's medium (DMEM, Gibco Inc., USA) supplemented with 10% v/v fetal bovine serum (FBS, Gibco), 2 mM glutamine (Himedia, India) and the antibiotics penicillin and streptomycin (Himedia) at recommended concentrations in a humidified atmosphere of 5% CO_2 at 37°C.

2.6.1 L-929 fibroblast cell adhesion studies

The polymer samples, each of size 1 cm^2 were placed in 24-well plates and exposed to UV light for 15 min. Fibroblast cells were seeded at a density of approximately 1×10^4 cells/ml and were incubated at 37°C, in 5% CO_2 atmosphere for 4 h. Following this, the medium was decanted and the polymer films were gently rinsed once with PBS. Cell adhesion and viability was determined using a dual staining method consisting of the membrane-permeant substrate carboxyfluorescein diacetate succinimidyl ester (CFDA SE) and the relatively membrane impermeant nuclear stain propidium iodide (PI) (Molecular Probes, Invitrogen). Briefly, the cells were stained with 5 μM CFDA SE and 500 nM of propidium iodide (PI) in phosphate buffered saline (PBS, pH 7.4) and were incubated at 37°C for 15 min. After incubation, the staining solution was decanted and the cells were subjected to further incubation for 30 min at 37°C in PBS containing 100 μg/ml DNase-free RNase. Cells were then washed with ice cold PBS and fixed with 4% paraformaldehyde. After mounting in Dako cytomation fluorescent mounting media (Dako, USA), the stained cells were examined under a confocal laser scanning microscope (Zeiss LSM 510, Germany) at 60× magnification. The numbers of adherent fibroblast cells present were counted from random fields selected across the polymer surfaces for all the samples. Statistical significance was ascertained by Student's t test and the data was expressed as means and SD from a single experiment performed in triplicates, which was representative of three independent experiments ($n = 3$ in each group).

2.6.2 RAW 264.7 macrophage cell adhesion studies

The polymer samples, each of size 1 cm^2 were placed in 24-well plates and exposed to UV light for 15 min. Mouse RAW 264.7 macrophage cells were seeded at a density of approximately 2×10^4 cells/ml and were incubated at 37°C, in 5% CO_2 atmosphere for 4 h. Initially, cells were stained using membrane-permeant substrate carboxyfluorescein diacetate succinimidyl ester (CFDA SE, Molecular Probes, Invitrogen). Briefly, the cells were stained with 5 μM CFDA SE in phosphate buffered saline (PBS, pH 7.4) and were incubated at 37°C for 15 min. After incubation, the staining solution was decanted and the cells

were subjected to further incubation for 30 min at 37°C in PBS containing 100 μg/ml DNase-free RNase (Fermentas). Cells were then washed with ice cold PBS and fixed with 4% paraformaldehyde. Fixed cells were rinsed twice with PBS and mounted in dako cytomation fluorescent mounting media containing propidium iodide (1 μg/ml) (Dako, USA). The number of adherent macrophages present were counted from random fields selected across the polymer surfaces for all the samples. Statistical significance was ascertained by Student's t test and the data was expressed as means and SD from a single experiment performed in triplicates, which was representative of three independent experiments ($n = 3$ in each group).

2.7 Real-time PCR analysis of pro-inflammatory cytokine gene expression

The inflammatory response to unmodified and the sulfobetaine modified PMMA films was evaluated with mouse RAW 264.7 macrophage cells by quantifying the expression levels of the secreted proinflammatory cytokines namely TNF-α and IL1-β after 4 h. The UV sterilized polymer films of size 1 cm^2 were placed in a 24-well plate and were incubated with RAW macrophage cells with a cell density of 2×10^4 cells/ml at 37°C, in 5% CO_2 atmosphere for 4 h, along with glass as control.

2.7.1 Total RNA extraction

The RNA of the samples taken from each time point was extracted from the cells with TRIzol®-reagent (Invitrogen, USA), as per the instructions of the manufacturer under RNase free conditions. The aqueous portion was extracted with chloroform and the subsequent RNA was precipitated with 70% ethanol in diethylpyrocarbonate treated water and then was purified with RNeasy column (Cat No. 74204, Qiagen). The concentrations of RNA were determined by UV spectrometry using Nanodrop ND-1000 (Thermo Scientific, USA). The quality of RNA was checked by means of denaturing formaldehyde agarose electrophoresis [36].

2.7.2 Deoxyribonuclease I (DNase I) treatment and reverse transcription (RT)

Prior to reverse transcription, all RNA samples were subjected to DNase I (Amersham Pharmacia) treatment at 37°C for 30 min, to remove genomic DNA contamination thereby preventing its carryover to the RT reaction. The samples were then mixed with 70% ethanol and further purified using RNeasy columns (Qiagen). The purified RNA was reverse transcribed using High Capacity cDNA Archive Kit (Applied Biosystems) according to the manufacturer's instructions [36].

Table 1 Primers used for the real-time PCR analysis

Gene target	Primer sequence	Orientation
TNF-α	5′-AGCCGATGGGTTGTACCTTGTCTA-3′	Forward
	5′-TGAGATAGCAAATCGGCTGACGGT-3′	Reverse
IL-1β	5′-TGTGAAATGCCACCTTTTGA-3′	Forward
	5′-CCTCTTCGACACCGTCGATG-3′	Reverse
GAPDH	5′-TGCACCACCAACTGCTTA-3′	Forward
	5′-GGATGCAGGGATGATGTT-3′	Reverse

2.7.3 Primer design

The mouse gene sequences were downloaded from NCBI database and the primers were designed using the IDT's SciTools Primer Quest [37]. Computational studies using the "blastn" software (http://www.ncbi.nlm.nih.gov/BLAST/) revealed that the designed primers (Table. 1) were unique for TNF-α, IL1-β and GAPDH (Glyceraldehyde 3 phosphate dehydrogenase). The primers, so generated were used in Real-Time PCR experiments.

2.7.4 Real-time PCR

Real-time PCR was performed using SYBR® Green PCR Master Mix using Applied Biosystem 7300 Real-Time PCR System. The PCR solution contained 2.5 μl of primer mix (final concentration, 166 nM), 7.5 μl of 2× SYBR PCR mix (Applied Biosystems, Foster City, CA), and 5 μl of the sample. Universal thermal PCR cycling conditions suggested by Applied Biosystems were followed and all samples were normalized to GAPDH. Statistical significance was ascertained by Student's t test and the data was expressed as means and SD from a single experiment performed in triplicates, which was representative of three independent experiments ($n = 3$ in each group).

3 Results

3.1 ATR–FTIR

The ATR–FTIR spectrum of the bare PMMA and PMMA-AC surfaces showed no obvious difference, indicating that solvent treatment have not changed the surface properties of base PMMA, however the spectrum of PMMA-SB film was notably different from the bare PMMA and PMMA-AC films in the region between 1040 and 1050 cm^{-1} region (Fig. 1). The IR spectrum of PMMA-SB showed appearance of a new sharp peak at 1040 cm^{-1} which could

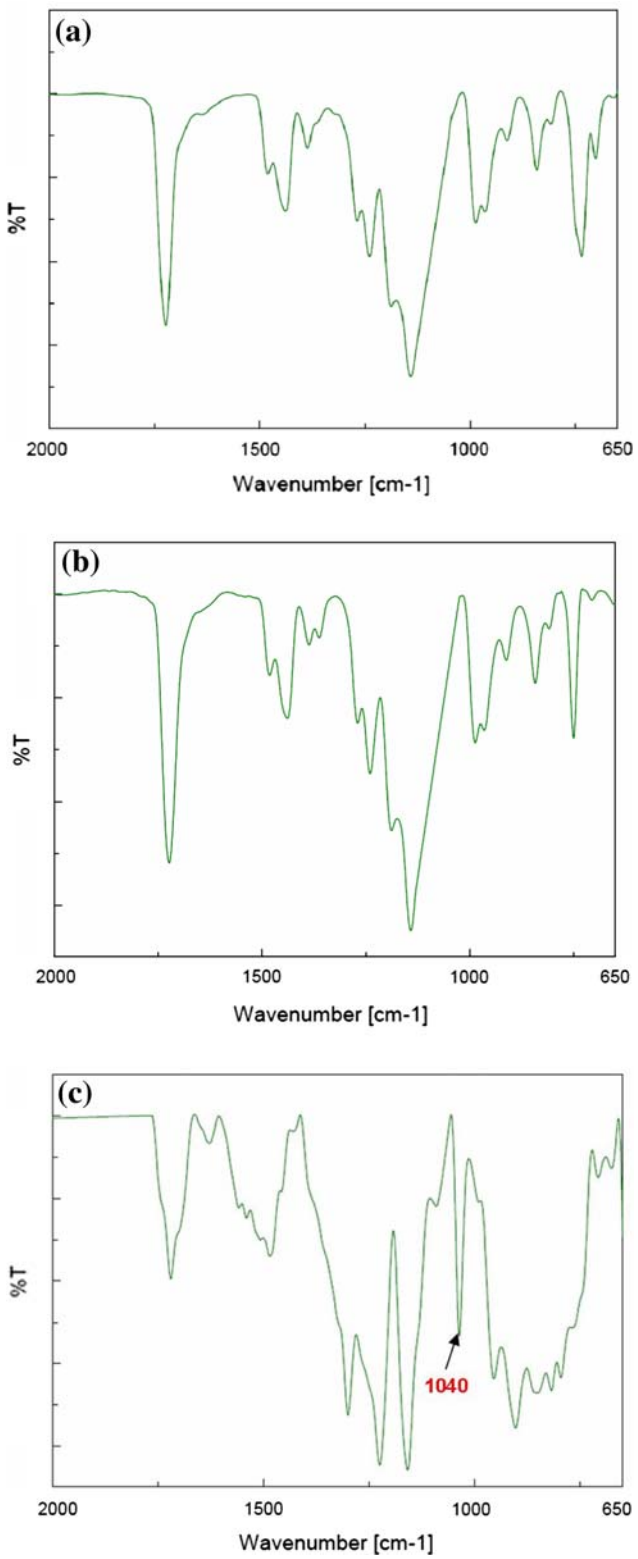

Fig. 1 ATR–FTIR spectra of **a** PMMA; **b** PMMA-AC and **c** PMMA-SB films

be assigned to the presence of SO_3^- vibrations in PMMA-SB films, indicating successful immobilization of sulfobetaine species on the PMMA surface.

3.2 Dynamic contact angle and surface free energy measurements

Both PMMA and PMMA-AC surfaces exhibited a typical hydrophobic nature characterized by relatively high values of advancing and receding contact angles (Table. 2). Immobilization of sulfobetaine molecules rendered the surfaces more hydrophilic, which was seen by reduction in the values of both θ_A and θ_R. The PMMA-SB surface showed much higher hysteresis than the base PMMA and PMMA-AC, indicating that its hydration leads to even more hydrophilic and wetted surface.

The total surface free energies and their dispersive and polar components were calculated according to the Fowkes's method and are presented in Table. 3. Overall, surface free energy of the sulfobetaine modified PMMA films showed an increase when compared to both the base PMMA and PMMA-AC surfaces. The polar (γ^p) component of the surface free energy significantly increased for PMMA-SB films compared to base PMMA and PMMA-AC substrates. In other words, the sulfobetaine modified films were more hydrophilic than the original films.

3.3 SEM–EDAX analysis

The changes in the chemical composition of the surface upon modification were also investigated by SEM–EDAX, which provided insight into the micro-space composition (Fig. 2). The elemental composition and the calculated O/C ratios of the modified and unmodified PMMA films are shown in Table 4. The spectra of base PMMA showed peaks for carbon (65.43%) and oxygen (20.07%), whereas the

Table 2 Dynamic contact angle analysis of the investigated PMMA surfaces

Polymer	Advancing contact angle (θ_A)	Receding contact angle (θ_R)	Hysterisis ($\theta_A - \theta_R$)
PMMA	77° ± 2.0	68° ± 3.0	9°
PMMA-AC	70° ± 2.7	60° ± 3.0	10°
PMMA-SB	59° ± 3.4	40° ± 4.0	19°

Values represent mean ± SD of five measurements ($n = 5$)

Table 3 Surface free energy and their components of the investigated PMMA surfaces

Sample	Dispersion component (γd) (mN/m)	Polar component (γp) (mN/m)	Surface energy (γ) (mN/m)
PMMA	23.15	14.10	37.25
PMMA-AC	22.30	15.45	37.75
PMMA-SB	15.84	25.47	41.31

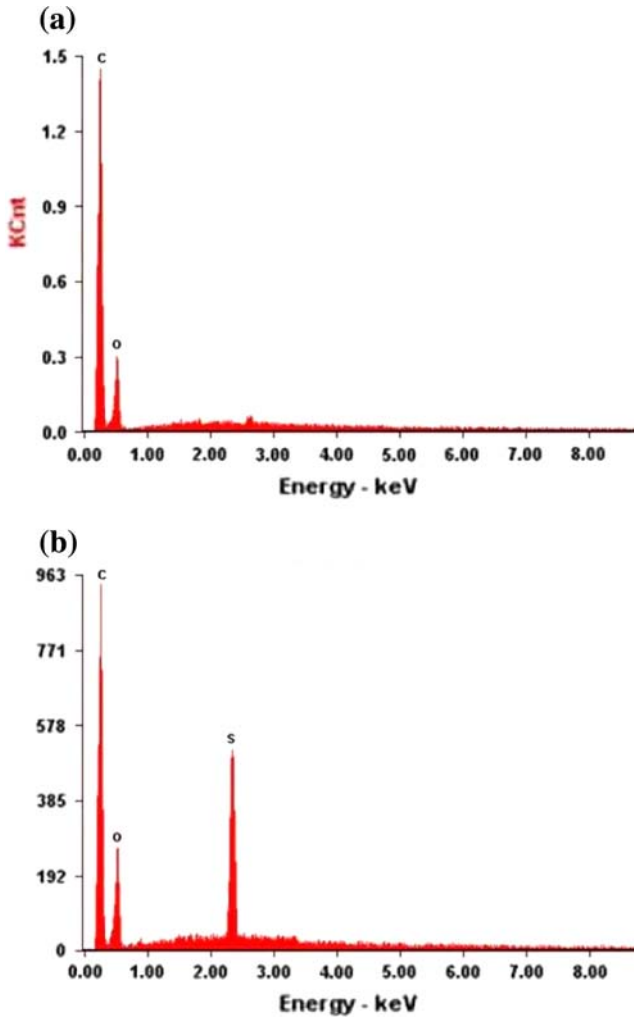

Fig. 2 SEM–EDAX analysis of **a** PMMA and **b** PMMA-SB films

Table 4 Surface elemental composition by EDAX of PMMA films modified with sulfobetaine species

Sample	Weight percent (%)			
	C	O	S	O/C
PMMA	65.43	20.07	–	0.30
PMMA-SB	67.08	22.71	4.66	0.33

sulfobetaine modified PMMA showed the additional peak for the presence of sulphur (4.66%). There was a significant increase in the O/C ratio upon sulfobetaine modification. Thus, SEM–EDAX results also indicated that sulfobetaine has been successfully immobilized onto PMMA surfaces.

3.4 Scanning electron microscopy investigation of entrapment structure

The cross-sectional part of the sulfobetaine modified PMMA film is shown in Fig. 3. It can be seen in the Fig. 3a

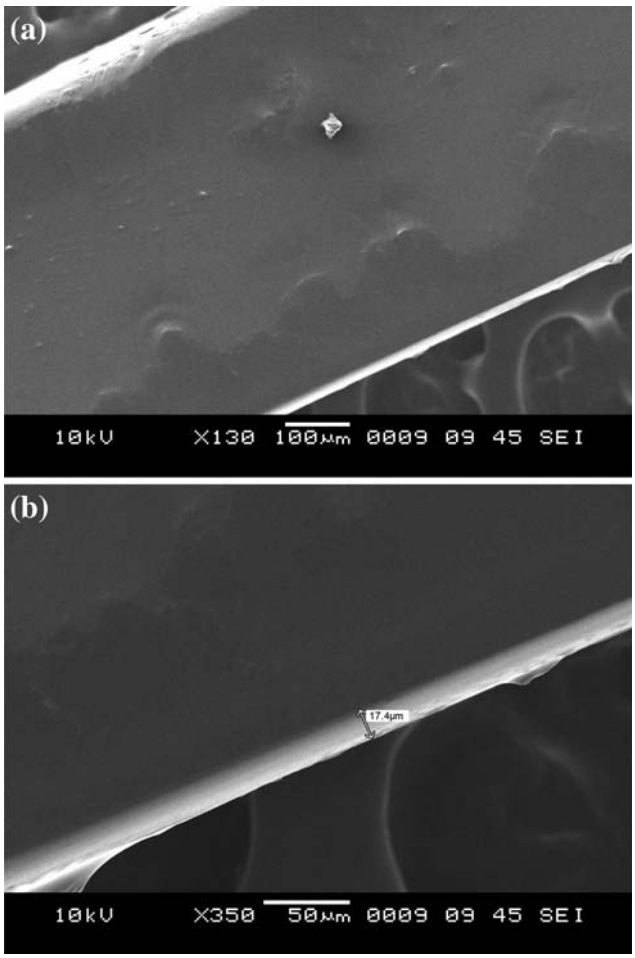

Fig. 3 Scanning electron microscopy investigation of cross-section part of the entrapment film. **a**, **b** SEM images of cross-sections of a sulfobetaine entrapped PMMA film

that both sides of the PMMA film were uniformly covered with sulfobetaine molecules. The thickness (depth) of the entrapped sulfobetaine layer was determined from Fig. 3b and was found to be approximately 15–17 µm, respectively.

3.5 Stability of surface films

Ultrasound treatment is a commonly used technique to desorb adsorbed species from surfaces [35]. A plot of the water contact angles versus the number of sonication cycles is shown in Fig. 4. It can be seen from the graph that in the case of PMMA with physically adsorbed sulfobetaine species, the water contact angle before sonication is 66.5°, but after the first sonication cycle it raises upto 75.6° and after second sonication cycle the contact angle is very similar to water contact angle of bare PMMA surface. This indicates that the sulfobetaine molecules are weakly adsorbed and not firmly bound to the PMMA surface and hence easily gets dislodged on sonication. On the other

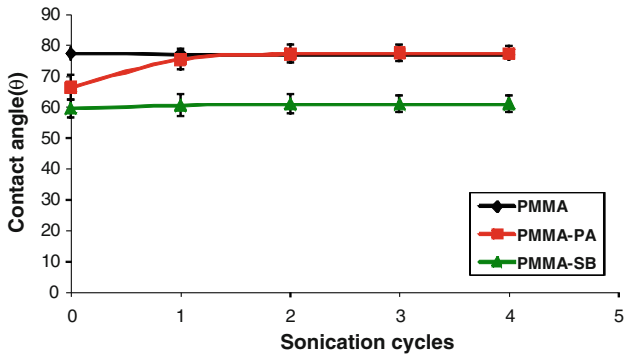

Fig. 4 Stability of the sulfobetaine modified PMMA films. Water contact angles versus sonication cycles. Values represent means ± SD from five measurements ($n = 5$)

hand, the water contact angles of PMMA-SB film remains at nearly constant values (around 61° ± 2) even after 4 sonication cycles which indicates that the sulfobetaine molecules are properly entrapped and are more stable on the PMMA surface than mere physical adsorption.

3.6 Protein adsorption

Material biocompatibility is generally considered to have relation with protein adsorption process, because adsorbed proteins may trigger both cellular adhesion and inflammatory events [35]. In the present work, unmodified and sulfobetaine modified substrates were studied in relation to adsorption of bovine fibrinogen in vitro. The adsorption of bovine fibrinogen (BFG) onto modified and unmodified PMMA surfaces from the protein solution (0.1 mg/ml) is shown in Fig. 5. There was no significant reduction in fibrinogen adsorption between solvent control PMMA-AC and the bare PMMA substrates ($P > 0.05$). However, adsorption of bovine fibrinogen was reduced by around 48% on PMMA-SB substrates as compared to the bare PMMA and by 43% compared to control PMMA-AC substrates respectively ($P < 0.05$). These results demonstrate that surface entrapment of sulfobetaine onto PMMA substrates could efficiently decrease fibrinogen adsorption.

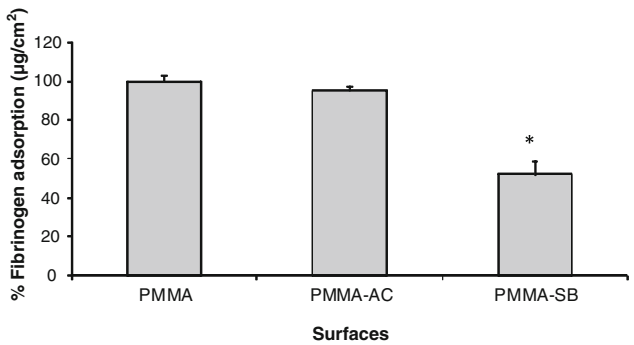

Fig. 5 Adsorption of bovine fibrinogen (BFG) onto the surface of modified PMMA films (*$P < 0.05$). Values represent means ± SD from a single experiment performed in triplicates, which was representative of three independent experiments ($n = 3$ in each group)

3.7 Short-term bacterial adhesion assays

Statistical analysis indicated that there was no significant reduction in adhesion of both the *S. aureus* and *P. aeruginosa* species between solvent control PMMA-AC and untreated PMMA substrates (Fig. 6a, b; $P > 0.05$). But, the PMMA-SB surface significantly reduced adhesion of both *S. aureus* and *P. aeruginosa* when compared to PMMA and PMMA-AC control (Fig. 6a, b; $P < 0.05$) after 4 h. Although the extent of reduction was found to be greater for *S. aureus* as compared to *P. aeruginosa.*

3.8 L-929 fibroblast adhesion studies

Two sample *t*-tests of the fibroblast adhesion data indicated that there was no significant reduction in fibroblast cell adhesion between solvent control PMMA-AC and untreated PMMA (Figs. 7 and 8; $P > 0.05$) substrates. However, significantly less fibroblast cells adhered to PMMA-SB than to bare PMMA and control PMMA-AC substrates (Figs. 7 and 8; $P < 0.05$). There was no

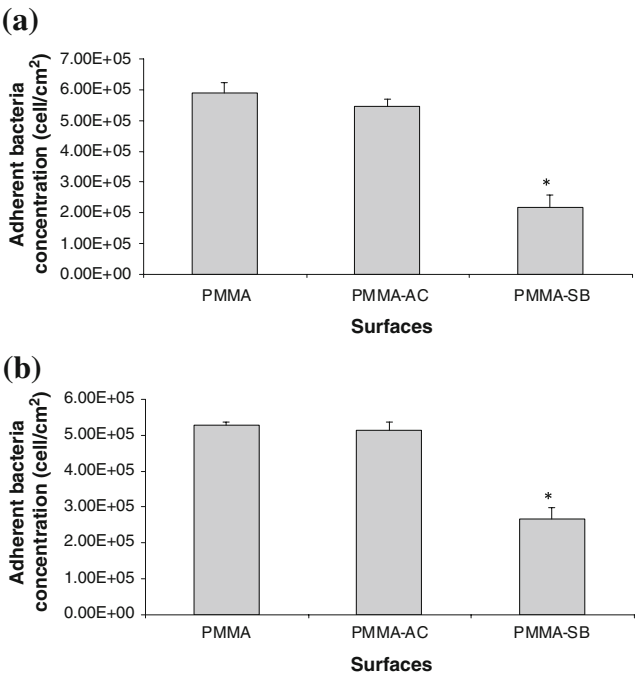

Fig. 6 Bacterial adhesion on materials incubated in approximately 1×10^8 cells/ml **a** *S. aureus* and **b** *P. aeruginosa* after 4 h (*$P < 0.05$). Values represent means ± SD from a single experiment performed in triplicates, which was representative of three independent experiments ($n = 3$ in each group)

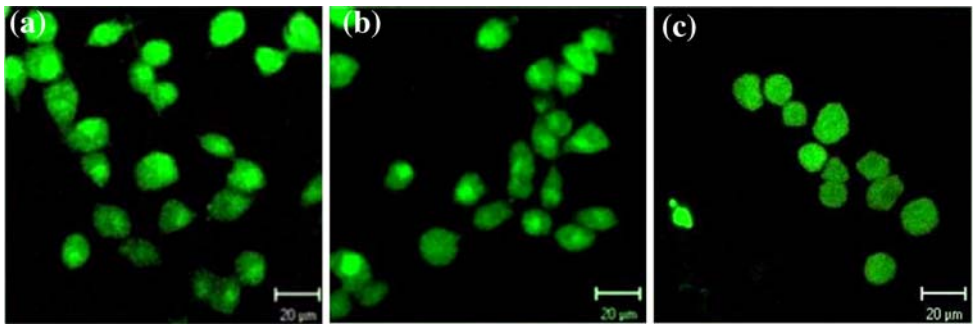

Fig. 7 Confocal laser scanning microscopy of L-929 fibroblast cell adhesion, after 4 h to **a** PMMA; **b** PMMA-AC and **c** PMMA-SB

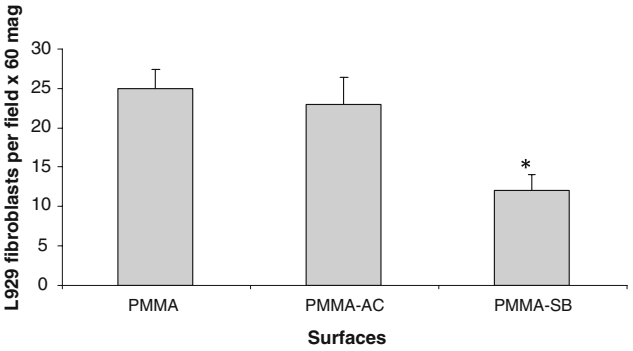

Fig. 8 L-929 mouse fibroblast adhesion to (a) PMMA; (b) PMMA-AC and (c) PMMA-SB incubated with approximately 1×10^4 cells after 4 h ($^*P < 0.05$). Values represent means ± SD from a single experiment performed in triplicates, which was representative of three independent experiments ($n = 3$ in each group)

evidence of material toxicity observed for the modified materials evaluated; as no PI staining was observed and the fibroblast cells were found to continue to grow on the tissue culture plastic wells containing the modified materials.

3.9 RAW 264.7 macrophage adhesion studies

Two sample t-tests of the macrophage adhesion data indicated that there was no significant reduction in macrophage adhesion between control PMMA-AC substrates and untreated PMMA (Figs. 9 and 10; $P > 0.05$). However, a significant reduction in adhesion of macrophages on PMMA-SB was observed when compared to PMMA and PMMA-AC control substrates (Figs. 9 and 10; $P < 0.05$).

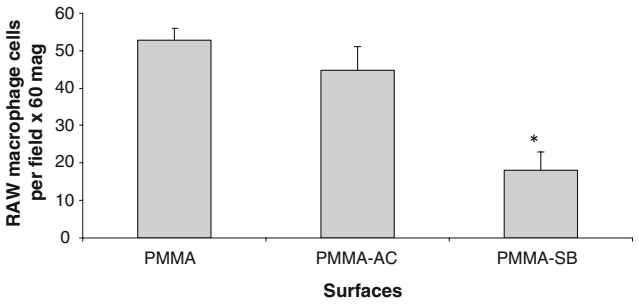

Fig. 10 RAW 264.7 macrophage cell adhesion to (a) PMMA; (b) PMMA-AC and (c) PMMA-SB incubated with approximately 1×10^4 cells after 4 h ($^*P < 0.05$). Values represent means ± SD from a single experiment performed in triplicates, which was representative of three independent experiments ($n = 3$ in each group)

3.10 Real-time PCR analysis of proinflammatory cytokine gene expression

The surface induced cellular inflammatory response to various polymers were evaluated by quantifying the expression levels of the proinflammatory cytokines namely TNF-α and IL1-β in RAW 264.7 macropahge cells after 4 h incubation, which was normalized to housekeeping gene GAPDH (Fig. 11). Macrophages exposed to PMMA had a nearly 15-fold increase in TNF-α expression, and a 10-fold increase in IL1-β expression which were the highest of all the samples. Whereas, cells exposed to PMMA-SB had a modest 1.9-fold increase in TNF-α ($^{**}P < 0.001$) and a 2.5-fold increase in IL1-β expression ($^{**}P < 0.001$) respectively.

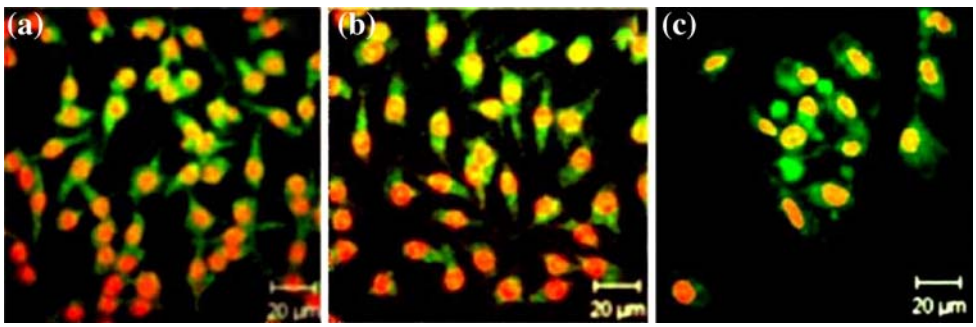

Fig. 9 Confocal laser scanning microscopy of RAW 264.7 macrophage cell adhesion, after 4 h to **a** PMMA; **b** PMMA-AC and **c** PMMA-SB

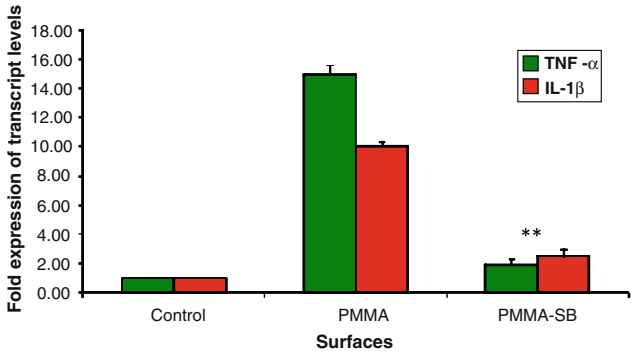

Fig. 11 Fold expression of TNF-α and IL-1β transcript levels after 4 h, as determined by real-time PCR analysis (**$P < 0.001$). Values represent means $\pm$ SD from a single experiment performed in triplicates, which was representative of three independent experiments ($n = 3$ in each group)

4 Discussion

In the recent past, various zwitterionic-based polymers have been shown to have biocompatible properties when used as coatings on medical devices [2, 38, 39]. Sulfobetaines are members of the zwitterionic betaine family of compounds which occur widely in nature. Betaines possess both positively and negatively charged groups within the molecule, but have an overall neutral charge. The sulfobetaine analogues are synthetically cheaper to produce than other zwitterionic ones and they can also be synthesized with good control over their architecture and molecular weight distribution, hence are potentially more attractive for a wider range of medical applications. About half of the Intraocular Lenses (IOLs) currently marketed are made from PMMA and its derivatives which are the major focus of this study. Sulfobetaine was used to modify the surface of PMMA by the entrapment method and its effect on various cell–material interactions was evaluated. The entrapment structure created by this solution technique led to a phase-mixed modifying species entangled in the base polymer (PMMA) and present at higher concentration near the polymer surface. The entrapment of sulfobetaine species on PMMA surface was quite stable as ultrasonication treatment was not able to desorb the entrapped sulfobetaine molecules from the PMMA-SB surface.

Protein adsorption is important in initial conditioning of the material when it is implanted into the body and is instrumental in activation of various inflammatory cascades and in providing adhesion sites for cells and bacteria on particular substrates [40, 41]. It is clear that plasma proteins have multifacet influences on the biocompatibility of different substrates that is probably determined by the ability of a particular surface to adsorb, denature and facilitate ligation of particular plasma proteins. Fibrinogen was used as a model protein since it adsorbs to a variety of surfaces. PMMA-SB surfaces were resistant to nonspecific fibrinogen adsorption while bare PMMA and solvent treated PMMA-AC surfaces showed high fibrinogen adsorption. Thus, radioactive ^{125}I labelled fibrinogen results confirmed previous findings of low protein adsorption on zwitterionic surfaces [42–45]. It is likely that the most effective biocompatible surface will be the surface on which associated proteins are retained in their native conformation. The PMMA-SB surface may achieve this through their ability to generate a hydrated surface that mimics the natural environment encountered by plasma proteins. The zwitterionic head group of sulfobetaine molecules has been shown to have a tendency to strongly bind water molecules leading perhaps to a thermodynamic hydration barrier [40, 42]. The differences between the PMMA-SB, PMMA-AC and bare PMMA polymers may be a consequence of their ability to bind water. The dynamic contact angle data would appear to support this, as the advancing contact angle for the PMMA-SB film was lower than both the PMMA-AC and bare PMMA films and also upon wetting reorientation and hydration occurs with PMMA-SB, as a result the hysteresis is much greater and the receding angle much lower suggesting a greater hydrophilicity and perhaps increased bound surface water. Thus the hydrated sulfobetaine chains existing on the PMMA-SB surface must alter the clear interface between PMMA-SB and water to a diffuse one.

The better performance of PMMA-SB substrates in reducing the adhesion of *S. aureus* and *P. aeruginosa* might be due to their ability to resist both the non specific protein adsorption and bacterial adhesion events. In addition there is clearly a difference in the adhesion of different types of bacteria to the PMMA-SB surface. This may reflect the differences in surface charges of the different organisms or their propensity to adhere to different extents to adsorbed proteins. Similarly, various research groups have previously demonstrated that coating of zwitterionic-based polymers, which mimic the phosphorylcholine headgroups and with their higher hydration capacity effectively repressed *S. aureus, Streptococcus mutans, P. aeruginosa* and *Candida albicans* attachment, thus findings of the present work are in general agreement with these reports [38–41].

The mouse L-929 fibroblast cell adhesion data shows a very clear advantage of PMMA-SB over bare PMMA in reducing cellular adhesion. It should also be noted that cellular adhesion is a cell-specific phenomenon that should be considered on a type-by-type basis. The results of RAW 267.4 macrophage cell adhesion shows that with the PMMA-SB surface have few adherent cells, and very few of those adhered cells being activated to secrete the pro-inflammatory cytokines TNF-α and IL1-β. Real-time PCR

analysis of the pro-inflammatory cytokines TNF-α and IL1-β production provided further confirmation that there were quantitative differences in the inflammatory response of RAW 264.7 macrophage cells to bare PMMA and PMMA-SB surfaces. Using the notion that an active macrophage cell produces greater amounts of given cytokines and/or chemokines, which is common in the study of biomaterial/cellular interactions, a cell can be defined as being in a more activated state than at previous time points or in comparison to other cells. The production of these cytokines, proteins by activated cells may influence the behaviors of other cells advancing a biological response (i.e., inflammation, the foreign body reaction). Adherent macrophages were investigated in our study for a material-dependency in the production of pro-inflammatory cytokines, which were then utilized to draw conclusions about the activation state of these cells. Previously, cellular activation was considered to correlate with cellular adhesion. The fewer number of cells that adhere to a particular surface, the less the overall activation of these cells [40, 46]. This was found to be true in the present study, in which decreasing RAW 264.7 macrophage cellular adhesion decreased the resulting inflammatory effects of these cells (i.e., cytokine production) concluding that these adherent cell populations are less active. Thus, the PMMA-SB surface has great advantage here, as it would be much less likely to initiate an inflammatory response than the bare PMMA. In addition reduced protein adsorption on the PMMA-SB substrates might also be an important factor, as it is generally believed that the ability to resist protein adsorption is a prerequisite for a surface to resist non specific adhesion events [47, 48]. This hypothesis has been tested by several research groups, and was also tested in the present study.

The zwitterionic nature of sulfobetaine molecules and the hydration of sulfobetaine based PMMA substrates are thought to be the reasons for their resistance towards non specific protein adsorption and cell/bacterial adhesion phenomenon. The surface electrical potentials arising from the zwitterionic structures may also contribute to the variation in proteins and cell adhesion through modification of the electrostatic interactions between the biological molecules and the surface. It is clear that further work is required to better understand the difference in the physicochemical and biological properties of these sulfobetaine modified polymers. Some potential applications where the use of sulfobetaine entrapment process on PMMA might be advantageous lie in areas of tissue contacting applications which involves materials in direct contact with tissues where non specific protein and cell adhesion is not desired, such as intraocular lenses (IOLs), biosensor membranes and other non fouling biomedical applications.

5 Conclusion

It is demonstrated by means of ATR–FTIR and SEM–EDAX analysis that sulfobetaine species can be immobilized on PMMA surface through entrapment by reversible swelling of the base polymer. Contact-angle measurements showed that the modified films were hydrophilic in nature. The performance of sulfobetaine modified PMMA surfaces in cell/serum environment demonstrated the success of this entrapment strategy, as the modified polymers showed better ability to inhibit protein adsorption and bacterial–cellular interactions at the PMMA surface. The inflammatory response as measured from the expression levels of pro-inflammatory cytokines TNF-α and IL-1β, were significantly lower upon exposure to modified films than that to bare PMMA. These studies have revealed that the sulfobetaine entrapment approach may potentially be used to create PMMA surfaces capable of preventing nonspecific adhesion events and suppress surface induced cellular inflammatory response. This entrapment strategy on PMMA would also be useful for applications in the fields of implanted devices and tissue engineering.

Acknowledgements The authors A.P. Khandwekar and D.P. Patil would like to thanks council of scientific and industrial research (CSIR) for providing fellowship for pursuing their doctoral studies.

References

1. Montargent B, Letourneur D. Toward new biomaterial. Infect Control Hosp Epidemiol. 2000;21:404–10.
2. Ishihara K. Novel polymeric materials for obtaining bloodcompatible surfaces. Trends Polym Sci. 1997;5:401–7.
3. Bridges AW, Singh N, Burns KL, Babensee JE, Lyon LA, Garcia AJ. Reduced acute inflammatory responses to microgel conformal coatings. Biomaterials. 2008;29:4605–15.
4. Anderson JM, Rodriguez A, Chang DT. Foreign body reaction to biomaterials. Semin Immunol. 2008;20:86–100.
5. Ratner BD, Bryant SJ. Biomaterials: where we have been and where we are going. Annu Rev Biomed Eng. 2004;6:41–75.
6. Ishihara K. Novel polymeric materials for obtaining blood compatible surfaces. Trends Polym Sci. 1997;5:401–7.
7. Chang CC, Merritt K. Effect of *Staphylococcus epidermidis* on adherence of *Pseudomonas aeruginosa* and *Proteus mirabilis* to polymethylmethacrylate (PMMA) and gentamicin containing PMMA. J Orthop Res. 1991;9:284–8.
8. Habash M, Reid G. Microbial biofilms: their development and significance for medical device-related infections. J Clin Pharmacol. 1999;39:887–98.
9. Gristina AG, Giridhar G, Gabriel BL, Naylor PT. Cell biology and molecular mechanisms in artificial device infections. Int J Art Organs. 1993;16:755–64.
10. Chang CC, Merritt K. Infection at the site of implanted materials with and without preadhered bacteria. J Orthop Res. 1994;12:526–31.
11. Dougherty SH. Pathobiology of infection on prosthetic devices. Rev Infect Dis. 1989;10:1102–17.

12. Sleigh JD. Changing patterns of bacterial and viral infections in surgery. Br Med Bull. 1998;44:403–22.
13. Kodjikian L, Burillon C, Chanloy C, Bostvironnois V, Pellon G, Mari E, et al. In vivo study of bacterial adhesion to five types of intraocular lenses. J Invest Ophthalmol Vis Sci. 2002;43:3717–21.
14. Cusumano A, Busin M, Spitzanas M. Is chronic intraocular inflammation after lens implantation of bacterial origin? Ophthalmology. 1991;98:1703–10.
15. Dilly PN, Holmes PJ. Bacterial adhesion to intraocular lenses. J Cataract Refract Surg. 1989;15:317–20.
16. Hayward JA, Chapman D. Biomembrane surfaces as models for polymer design the potential for hemocompatibility. Biomaterials. 1984;5(3):135–42.
17. Ishihara K, Nakabayashi N, Sakakida M, Nishida K, Shichiri M. Biocompatible microdialysis hollow-fiber probes for long-term in vivo glucose monitoring. In: Akmal N, Usmani A, editors. Polymers in sensors: theory and practice. ACS symposium series, vol. 690. Washington, DC: American Chemical Society; 1998.
18. Ishihara K, Oshida H, Endo Y, Wanatabe A, Ueda T, Nakabayashi N. Effects of phospholipid adsorption on nonthrombogenicity of polymer with phospholipid polar group. J Biomed Mater Res. 1993;27:1309–14.
19. Ishihara K. New polymeric biomaterials-phospholipid polymers with a biocompatible surface. Front Med Biol Eng. 2000;10:83–95.
20. Lewis AL, Hughes PD, Kirkwood LC, Leppard SW, Redman RP, Tolhurst LA, et al. Synthesis and characterisation of phosphorylcholine-based polymers useful for coating blood filtration devices. Biomaterials. 2000;21:1847–59.
21. Lewis AL. Phosphorylcholine-based polymers and their use in the prevention of biofouling. J Colloids Surf. 2000;18:261–75.
22. Watanabe A, Kojima M, Ishihara K, Nakabayashi N. Interaction of platelets and cultured cells with polymers containing phospholipid polar groups, vol. 23. Reports of the Institute for Medical and Dental Engineering, Tokyo Medical and Dental University; 1989. p. 31–9.
23. McCormick CL, Salazar LC. Water-soluble copolymers. Amopholytic copolymers of sodium 2-(acrylamido)-2-methylpropanesulfonate with [2-(acrylamido)-2-ethylpropyl]trimethylammonium chloride. Polymer. 1992;33:4617–24.
24. Monroy VM, Galin JC. Poly(sulphopropylbetaines): 2. Dilute solution properties. Polymer. 1984;25:121–5.
25. Salamone JC, Volksen W, Israel SC, Olson AP, Raia DC. Preparation of inner salt polymers from vinylimidazolium sulphobetaines. Polymer. 1977;18:1058–62.
26. Liaw DJ, Lee WF, Whung YC. 3-Dimethyl(methacryloyloxyethyl) ammonium propane sulfonate. J Appl Polym Sci. 1987;34:999–1011.
27. Khandwekar AP, Patil DP, Khandwekar V, Shouche YS, Sawant S, Doble M. TecoflexTM functionalization by curdlan and its effect on protein adsorption and bacterial and tissue cell adhesion. J Mater Sci: Mater Med. 2009;20:1115–29.
28. Khandwekar AP, Patil DP, Shouche YS, Doble M. Controlling biological interactions with surface entrapment-modified polyurethane. J Med Biol Eng. 2009;29:84–91.
29. Khandwekar AP, Patil DP, Shouche YS, Doble M. The biocompatibility of sulfobetaine engineered poly(ethylene terepthalate) by surface entrapment technique. J Biomater Appl. 2009. doi:10.1177/0885328209344004.
30. Goodman SB. Does the immune system play a role in loosening and osteolysis of total joint replacements? J Long Term Eff Med Implants. 1996;6(2):91–101.
31. Bustin SA. Absolute quantification of mRNA using real-time reverse transcription polymerase chain reaction assays. J Mol Endocrinol. 2000;25(2):169–93.
32. Glu GB, Arıca MY. Surface energy components of a dye-ligand immobilized pHEMA membranes: effects of their molecular attracting forces for non-covalent interactions with IgG and HSA in aqueous media. Int J Biol Macromol. 2005;37:249–56.
33. Russ IG. Energy dispersive X-ray analysis, the scanning electron microscope in energy dispersive X-ray analysis, STP, 485, American Society for Testing and 154, Philadelphia; 1971.
34. Egyhazi T, Scholtz J, Beskov VS. SEM–EDAX investigations of use-related microstructural changes in an ammonia synthesis catalyst. React Kinet Catal Lett. 1984;24:1–8.
35. Venugopal B, James T, Nirmala R, Jayakrishnan A. A photochemical method forimmobilization of azidated dextran onto aminated poly(ethylene terephthalate) surfaces. Polym Int. 2008;57:124–32.
36. Leong DT, Gupta A, Bai HF, Wand G, Yoongd LF, Tood HP, et al. Absolute quantification of gene expression in biomaterials research using real-time PCR. Biomaterials. 2007;28:203–10.
37. Harris TH, Cooney NM, Mansfield JM, Paulnock DM. Signal transduction, gene transcription, and cytokine production triggered in macrophages by exposure to trypanosome DNA. Infect Immun. 2006;74:4530–7.
38. Hayward JA, Chapman D. Biomembrane surfaces as models for polymer design: the potential for haemocompatibility. Biomaterials. 1984;5:135–42.
39. Hirota K, Murakami K, Nemoto K, Miyake Y. Coating of a surface 2-methacrylo-phosphorylcholine (MPC) co-polymer significantly reduces retention of human pathogenic microorganisms. FEMS Microbiol Lett. 2005;248(1):37–45.
40. West SL, Salvage JP, Lobb EJ, Armes SP, Billingham NC, Lewis AL, et al. The biocompatibility of crosslinkable copolymer coatings containing sulfobetaines and phosphobetaines. Biomaterials. 2004;25:1195–204.
41. Cheng G, Zhang Z, Chen S, Bryers JD, Jiang S. Inhibition of bacterial adhesion and biofilm formation on zwitterionic surfaces. Biomaterials. 2007;28:4192–9.
42. Zhang Z, Chen SF, Chang Y, Jiang SY. Surface grafted sulfobetaine polymers via atom transfer radical polymerization as superlow fouling coatings. J Phys Chem B. 2006;110(22):10799–804.
43. Chen SF, Yu FC, Yu QM, He Y, Jiang SY. Strong resistance of a thin crystalline layer of balanced charged groups to protein adsorption. Langmuir. 2006;22(19):8186–91.
44. Li LY, Chen SF, Zheng J, Ratner BD, Jiang SY. Protein adsorption on oligo(ethylene glycol)-terminated alkanethiolate self-assembled monolayers: the molecular basis for nonfouling behavior. J Phys Chem. 2005;109(7):2934–41.
45. Chen SF, Li LY, Boozer CL, Jiang SY. Controlled chemical and structural properties of mixed self-assembled monolayers of alkanethiols on Au. Langmuir. 2000;16(24):9287–93.
46. Krishna OD, Kim K, Byun Y. Covalently grafted phospholipid monolayer on silicone catheter surface for reduction in platelet adhesion. Biomaterials. 2005;26:7115–23.
47. Ratner BD, Hoffmann FJ, Schoen JE, Lemons F. Biomaterials science: an introduction to materials and medicine. New York, NY: Academic Press; 1996.
48. Chapman RG, Ostuni E, Liang MN, Meluleni G, Kim E, Yan L, et al. Polymeric thin films that resist the adsorption of proteins and the adhesion of bacteria. Langmuir. 2001;17(4):1225–33.